Optical Fiber Technology **6,** 122–154 (2000)
doi:10.1006/ofte.2000.0327, available online at http://www.idealibrary.com on IDEAL®

Invited Paper

Theory and Measurement Techniques for the Noise Figure of Optical Amplifiers

Douglas M. Baney

Agilent Laboratories, 3500 Deer Creek Road, Palo Alto, California 94304

Philippe Gallion

Ecole Nationale Superieure des Telecommunications, 46 rue Barrault, Paris Cedex 13, France

and

Rodney S. Tucker

Australian Photonics Cooperative Research Centre, Department of Electrical and Electronic Engineering, University of Melbourne, Parkville, Victoria 3052, Australia

Received December 29, 1999

The theoretical basis for the noise figure of optical amplifiers is reviewed, and a consistent approach to determining the noise figure of cascaded components is developed. It is shown that when the noise figure is defined in terms of the input and output signal-to-noise ratios, the formulation provides a consistent theoretical formulation for measurement techniques using optical and optoelectronic measurement methods. The paper concludes with a review of measurement techniques for characterization of the noise figure.

I. INTRODUCTION

Optical amplifiers are used extensively in optical fiber telecommunications. By injecting laser pump light at a wavelength of 980 or 1480 nm into a strand of erbium-doped optical fiber, high optical gain at wavelengths between 1.5 and 1.6 μm can be obtained [1]. Erbium-doped fiber amplifiers (EDFAs) routinely amplify dozens of wavelengths simultaneously to compensate for signal power losses due to

1068-5200/00 $35.00

splitting and propagation through optical fiber. In addition to providing optical gain, amplifiers also add undesired optical power fluctuations onto the signal. This intensity noise can lead to poor signal reception in analog communications or high bit-error rates in digital transmission systems [2]. In electronic amplifiers, it is common to quantify the effects of noise using a parameter known as the noise figure. This concept of a noise figure can also be applied to optical amplifiers [1–5], but it should be noted that not all definitions in the literature are the same. The purpose of the present paper is to present a consistent approach to modeling the noise figure of optical amplifiers and other optical components and to review noise figure measurement techniques.

The undesired optical power fluctuations (intensity noise) introduced by optical components cause transmission impairments in optical communications systems. This noise can be characterized indirectly by measuring the optical field power spectrum and using an approximate model to evaluate the intensity noise. Alternatively, optoelectronic detection is used where a photodetector converts the optical power into an electrical signal and the accompanying noise is analyzed using standard electronic techniques. Characterization of the noise figure of an optical amplifier can be straightforward or complicated depending on the context in which the noise figure data are employed. For the simple situation where the noise figure is used to quantify the contribution of the EDFA to the accumulation of amplified spontaneous emission (ASE) in a cascade of amplifiers, optical measurement methods are commonly used. In cases where the complete noise figure is required, such as when optical reflection-induced intensity noise must be considered, optoelectronic measurement methods should be used. The model presented here applies to both optical and optoelectronic noise figure measurement techniques. Reduced to its simplest form, it is shown to be consistent with the noise figure as defined by the IEC (SC86C, Working Group 3), the international standards body responsible for optical amplifier noise figure definitions. That definition has been adopted by the ITU-T (International Telecommunications Union—Telecommunications) and is in use by the major test instrument and optical amplifier equipment manufacturers [6].

The paper is structured as follows. We begin with a discussion of noise figure in optical amplifiers and other optical components. In Section II we present a model of noise in optical two-port devices. Section III defines the optical noise figure, which is then cast in terms of measurable parameters in Section IV. The expected ASE at the end of an amplifier cascade is derived in Section V. Section VI reviews various optical and optoelectronic techniques for noise figure measurement.

II. INTENSITY NOISE

The principle sources of transmission impairment in intensity-modulated communications systems are timing jitter and intensity noise [2, 5]. EDFAs can contribute significantly to intensity noise degradation resulting in vertical closure of the eye pattern of detected intensity-keyed signals as viewed on an oscilloscope. The effect of intensity noise is illustrated in Fig. 1. The transmitter output shown in

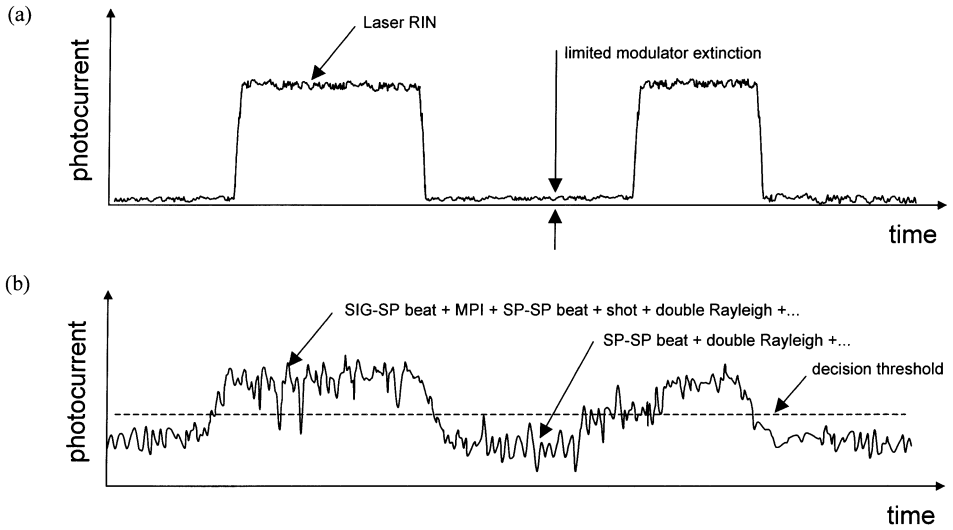

FIG. 1. Signal degradation due to amplifier produced noise: (a) Transmitter output with SNR as limited by laser RIN. (b) Received signal corrupted by beat, multipath interference and shot noise.

Fig. 1a has a good signal-to-noise ratio (SNR) which is limited by the excess relative intensity noise (RIN) or shot noise of the transmitter laser. After traversing an optical network composed of transmission fiber and optical amplifiers, the SNR becomes degraded, as shown in Fig. 1b. This increases the errors generated by decision circuits that determine whether a logical "1" or "0" was transmitted. Contributions to intensity noise include [1–3, 5–12]:

- Signal-spontaneous (sig-sp) beating
- Spontaneous-spontaneous (sp-sp) beating
- Multipath interference (MPI)
- Amplified double-Rayleigh backscatter
- Shot noise due to signal, ASE, and the remnant pump light.

Figure 1b indicates which of these contribution affect the logical "1" and "0" levels.

Figure 2 shows the distributions of some of the intensity noise sources inherent to the optical amplifier. Figure 2a shows the distributions of the optical field spectrums $S_E(\nu)$ and the associated signal-spontaneous beating, which originates from the mixing or beating of the coherent signal with the incoherent ASE in the same polarization. The curve on the left of Fig. 2a is the optical field power spectrum (measurable with an optical spectrum analyzer) and the curve on the right is the intensity spectrum (measurable using a photodetector and an electrical spectrum analyzer). Note that ν is the frequency of the optical field and f is the baseband frequency of the electrical output from the photodetector. For reference, very approximate values of optical frequency and baseband frequency are given in

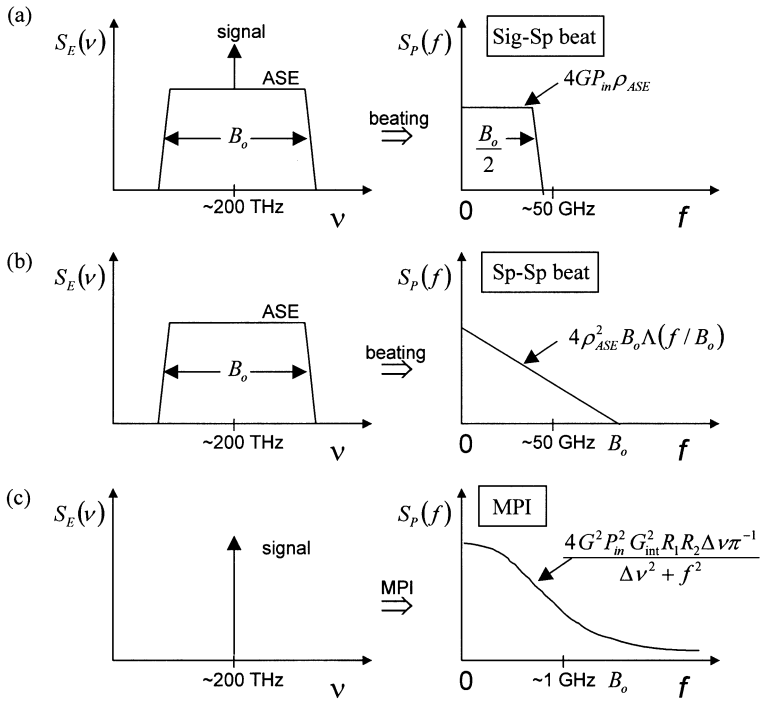

FIG. 2. Distributions of some of the intensity noise sources created by the optical amplifier. $S_E(\nu)$ optical field power spectrum, $S_P(f)$ intensity spectrum.

Fig. 2. Note that the bandwidth of the intensity spectrum shown here is limited to about 50 GHz by optical filtering after the amplifier. (The optical bandwidth is B_o.)

Figure 2b shows the optical field power spectrum and the intensity spectrum of sp-sp beat noise [1–3, 5, 7]. Beating of copolarized spectral components of ASE causes sp-sp beat noise. This noise is also dependent on the baseband frequency, with the noise density decreasing with increasing baseband frequency, f. In principle, the spontaneous–spontaneous intensity spectrum could be as wide as the optical amplifier bandwidth (> 5000 GHz) in the absence of optical filtering, but this would generally not be measurable due to the limited bandwidth of practical photodetectors and electrical spectrum analyzers.

Figure 2c illustrates another important intensity noise known as MPI noise. MPI noise arises from the conversion of phase or frequency noise associated with the signal to intensity noise. This occurs within optical amplifiers. Figure 3 shows the structure of a typical EDFA. The various components (e.g., isolators, multiplexers, erbium-doped fiber) that constitute the optical amplifier contribute optical reflections in the signal path. These reflections are highlighted in Fig. 3. In a manner similar to a frequency discriminator, these reflections convert signal phase and frequency fluctuations into intensity noise. Optical reflections may also enhance ASE production by the amplifier. The expected intensity noise is shown in Fig. 2c for two reflections situated on either side of internal gain, G_{int}. G gives the amplifier net gain, and the laser linewidth (Lorentzian) $\Delta\nu$ is such that the time

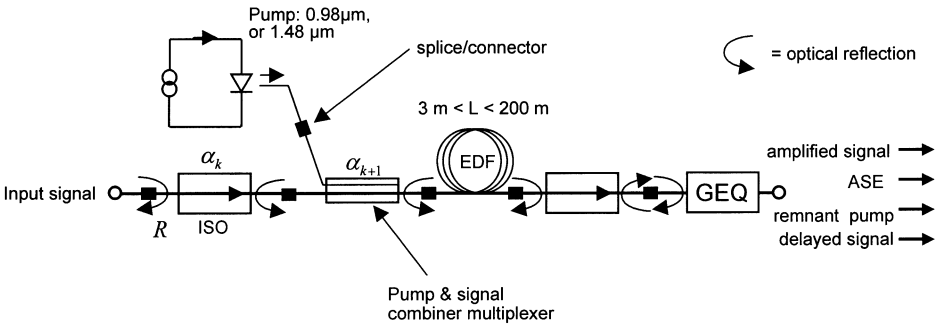

FIG. 3. A simple erbium-doped fiber optic amplifier showing its basic components. Components have optical reflections R and attenuation α_k that contribute to the noise generated by the amplifier. ISO, optical isolator; EDF, erbium doped fiber; GEQ, gain equalizer; ASE, amplified spontaneous emission.

delay between the reflections exceeds the coherence time of the laser [3]. In practice, the time delay may not always exceed the coherence time and multiple reflections of unknown strengths and polarizations can interfere. MPI noise is baseband frequency-dependent and is of particular importance when optical amplifiers are used for CATV, sensing, and high-frequency subcarrier transmission [12]. Another important effect is simulated Brillouin backscatter (SBS), which is due to acoustic waves in optical fiber caused by a strong optical signal field. SBS is known to cause significant baseband frequency noise with a peak around 11 GHz [3]. Even the intrinsic molecular level variations of the index of refraction of glass causes reflections, known as Rayleigh backscatter, that can contribute significant noise in high gain amplifiers [10, 11].

The noise sources described above can be categorized into a noise grouping known as excess noise. This is illustrated in Fig. 4, which shows schematically how the noise level can lie anywhere between zero and infinity, depending on the noise source and the optical attenuation. In the squeezed regime [13, 14], the noise level of an optical signal at a given power level is less than the shot noise that would normally be associated with a signal at that power level. The noise level of a squeezed signal typically increases (relative to the signal level) in the presence of optical attenuation. As the attenuation increases, the noise level approaches the

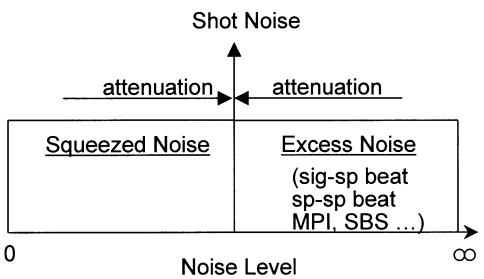

FIG. 4. Regimes of noise level relative to signal power. In the presence of optical attenuation, all noise converges to shot noise.

usual shot noise level associated with a signal of that power level. Of greater practical significance than the squeezed noise regime is the excess noise regime. In this regime, the noise level is higher than the level of shot noise, due to the influence of excess noise sources such as signal–spontaneous beat noise, etc. In the excess noise regime, the noise decreases with increasing attenuation and converges to pure shot noise.

Given the number of different noise sources, and the fact that the importance of the individual noise sources varies with the application and design of the amplifier, a correct definition of noise figure should include all contributions to noise. The noise figure formulation provided in this paper is based on a general description of the SNR degradation of intensity modulated signals used in direct detection optical systems that are currently in widespread use. The approach presented here is valid for all types of intensity noise.

III. NOISE FIGURE—DEFINITION

Signal-to-Noise Ratio

Prior to defining the noise figure, we will define the SNR, which forms the basis of optical amplifier and optical component noise figure calculations. The SNR serves as a measure of the quality of a signal. It is determined in terms of the signal and noise levels in the photocurrent of a photodetector placed in the signal path. The SNR can be calculated in terms of the received signal photocurrent, i_{sig}, and the variance of the received photocurrent noise $\langle \Delta^2 i_n \rangle$.

$$SNR = \frac{\langle i_{\text{sig}} \rangle^2}{\langle \Delta^2 i_n \rangle}, \tag{1}$$

where the noise variance $\langle \Delta^2 i_n \rangle$ is found by integrating the received intensity noise spectrum over the bandwidth of interest [3].

$$\langle \Delta^2 i_n \rangle = \Re^2 \int_{B_e} S_P(f)\, df, \tag{2}$$

where $S_P(f)$ is the power spectral density of the undesired power fluctuations accompanying the signal, B_e is the photodetector bandwidth, $\Re$ is the photodetector responsivity with units of amps/watt, and f is the electrical baseband frequency. Note that the SNR is defined in terms of a ratio of power levels of the photocurrent. Thus the SNR is a ratio of electrical power levels rather than a ratio of optical power levels.

Noise Figure

Just as the SNR serves as a figure of merit to characterize the noise quality of a signal, the noise generation nature of optical amplifiers or other components can be characterized by the noise figure of the component. The noise figure enables

system and component designers to evaluate the impact of a component on the SNR of a signal passing through that component. Noise figure quantifies the degradation of the SNR due to the insertion of an amplifier or component in a signal transmission. Noise figure thus reflects the impact of the diversity of noise sources that impact the overall noise performance of the amplifier or component.

We begin by defining the noise factor. Using the nomenclature of the IEC, [IEC 61291-1], the noise factor F is defined by

$$F(\nu, f) = \frac{SNR_{\text{in}}}{SNR_{\text{out}}(\nu, f)}, \tag{3}$$

where SNR_{in} is the SNR at the amplifier input and SNR_{out} is the SNR at the output. In general, noise factor is a function of both the optical frequency ν and the baseband frequency f [3, 8, 12]. In order to provide consistency and repeatability, it is necessary that SNR_{in} is fixed and known. We return to this important issue below, where we discuss the choice of the input noise reference signal used in the measurements.

The noise figure (NF) is the noise factor expressed in decibel units:

$$NF = 10\log_{10}(F). \tag{4}$$

This notation is used through this article to be consistent with IEC usage. The noise factor in Eq. [4] is consistent with the definition of SNR as a ratio of detected photoelectric power levels. Thus the NF is expressed correctly in electrical dB rather than in optical dB.

The general concept of noise figure measurement is illustrated in Fig. 5. Essentially, noise figure describes the SNR degradation when the component is inserted at specified measurement reference planes and boundary conditions. In

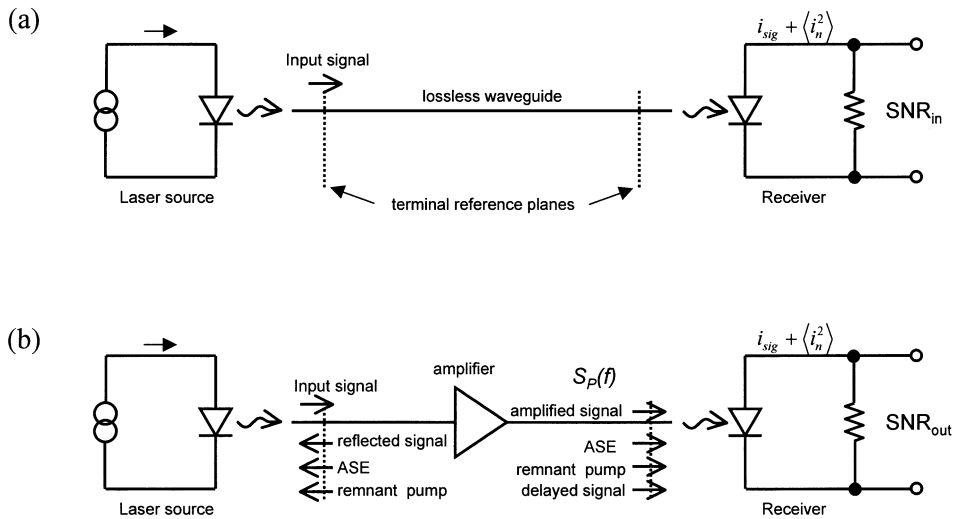

FIG. 5. Noise figure is defined as the ratio of input to output SNRs for an ideal receiver when illuminated by a shot-noise-limited source. (a) Measurement of input SNR, SNR_{in}; (b) Measurement of output SNR, SNR_{out} showing sources of noise from optical amplifier.

practice, this can be achieved using a receiver that measures the input SNR, SNR_{in}, and the output SNR, SNR_{out}, using a substitution method. To be useful, it is important that measurements of noise figure are independent of the nonidealities of the system used in its characterization. This point is quite important since it greatly affects the methods used to characterize the amplifier. If noise figure measurements could not be separated from the characteristics of individual test setups, then it would be difficult to compare results between different testing laboratories. For this reason the test setup must use ideal sources and receivers; if not, a correction for the source and receiver nonidealities is required. We will return to this in Section VI, where we review NF measurement techniques.

Input Noise Reference Signal

We now look at the choice of an input reference signal for use in noise figure measurements and calculations. Okoshi and Kikuchi [2] defined noise figure in terms of a coherent input reference signal without any excess noise. In other words, their definition uses a shot-noise-limited input reference. The shot-noise-limited input reference is widely used in the literature [1–3, 5, 6, 12, 15–21], it has been implemented by the noise figure instrument makers [20], and it is incorporated into the international definition of noise figure by the IEC [IEC 61291-1].

Since shot noise arises from the particulate nature of uncorrelated photons or electrons. It represents the minimum practical noise (ballistic transport regime) obtainable in photonic or electronic circuits. An additional feature of the shot noise reference is that any signal will become shot-noise limited with sufficient attenuation. This feature has proven very useful in amplifier testing when only lasers with excess noise (beyond shot noise) are available for measurement [3].

In principle, it would be possible to use squeezed light as an input noise reference signal. As pointed out earlier, it is possible to obtain a noise level below shot noise through squeezing [13, 14]. This is the so-called nonclassical intensity-squeezed light. The degree of squeezing is rapidly lost if any loss (or gain) is present in the propagation path. Due to the delicate nature of squeezed light with respect to absorption, we believe that it does not provide a convenient measurable input noise reference.

A third alternative for the input noise reference is to use a signal with a known amount of excess noise. This approach is analogous to the noise figure definition used in electrical circuits, where the input reference signal is based on thermal noise at a room temperature of 290 K. A significant disadvantage of using excess noise as a reference in noise figure measurements on low-noise optical components such as amplifiers is that the excess noise at the input can mask the noise produced by the amplifier under test. A consequence of this is a reduction in the accuracy of noise figure measurements that use excess noise at the input.

IV. NOISE FIGURE IN TERMS OF MEASURABLE PARAMETERS

In this section we explore the detailed noise figure characteristics of optical amplifiers and other optical components. We begin with the input and output SNR.

Input SNR

As discussed above, the input signal is defined to be shot-noise-limited. Its signal-to-noise ratio SNR_{in} is measured as shown in Fig. 5, and the measured SNR for a shot-noise-limited source is given by [1–3]

$$SNR_{\text{in}} = \frac{\langle i_{\text{in}} \rangle^2}{\langle \Delta^2 i_n \rangle} = \frac{\Re^2 P_{\text{in}}^2}{2q\Re P_{\text{in}} B_e} = \frac{\eta P_{\text{in}}}{2h\nu B_e}, \tag{5}$$

where i_{in} is the photocurrent generated by the optical signal of power level P_{in}. The photodetector responsivity is $\Re = \eta q/h\nu$ where η is the photodetector quantum efficiency and B_e is the baseband bandwidth of the noise. The term $\langle i_{\text{in}} \rangle^2$ in the numerator of Eq. (5) is proportional to the detected electrical signal power and the $\langle \Delta^2 i_n \rangle$ term in the denominator is the mean-square value of a single-sided noise power spectrum. Equation (5) shows that the detected signal power depends on the square of P_{in} and that the shot noise is proportional to P_{in}. Note that SNR_{in} depends on the quantum efficiency of the receiver. The noise factor defined below assumes an ideal receiver, which means that it is usually necessary to calibrate the receiver and numerically correct for the nonunity quantum efficiency. For an ideal receiver with negligible thermal noise, and a noise bandwidth B_e of 1 Hz, Eq. (5) becomes

$$SNR_{\text{in}} = \frac{P_{\text{in}}}{2h\nu}. \tag{6}$$

An alternative approach to deriving Eq. (5) is by adding the so-called zero point fluctuations, N, with a single-sided spectral density of $h\nu/2$, to a classical signal A_o normalized such that $|A_o|^2$ is the optical power P_{in}. The resulting instantaneous optical power fluctuations are $|(A_o + N)|^2 \approx P_{\text{in}} + 2AN_i$ where N_i is the in-phase component of N. Note that the bandwidth associated with N is twice the baseband bandwidth for the in-phase and the quadrature components and these two components equally share the total noise power for the coherent (nonsqueezed) light ascribed to the shot-noise-limited signal. The power fluctuation $\Delta P_{\text{in}} = 2AN_i$ has an associated power spectrum of $2h\nu$ that is four times the zero-point fluctuations.

Output SNR

The output noise depends on a number of contributing noise sources, with differing spectral densities and with differing significance depending on the context within which the amplifier is used. Since the output signal-to-noise ratio is based on measurable optical power levels and not optical field quantities, it can be measured in an identical way to the (reciprocal) RIN used to describe laser noise [2, 3, 17]. The output SNR is often normalized to a 1 Hz bandwidth as with the input SNR, which also makes it consistent with the common usage of RIN.

The output signal-to-noise ratio is given by

$$SNR_{\text{out}} = \frac{\langle i_{\text{out}} \rangle^2}{\langle \Delta^2 i_{\text{out}} \rangle}, \tag{7}$$

where

$$\langle i_{\text{out}} \rangle^2 = \Re^2 G^2 P_{\text{in}}^2.$$

The most direct approach to determine the denominator of Eq. (7) is to simply add the intensity noise power spectral densities of all the contributing uncorrelated noise sources. The measured output SNR then becomes

$$SNR_{\text{out}} = \frac{\Re^2 G^2 P_{\text{in}}^2}{B_e \Re^2 \left[S_{\text{sig-sp}} + S_{\text{sp-sp}} + S_{\text{MPI}} + S_{\text{pump}} + \cdots + \eta^{-1} S_{\text{shot}} \right]}, \tag{8}$$

where G is the optical gain of the amplifier and $S_{\text{sig-sp}}$, $S_{\text{sp-sp}}$, S_{MPI}, S_{pump}, and S_{shot} are the baseband noise spectral densities of signal-spontaneous beat noise, spontaneous–spontaneous beat noise, multipath interference noise, pump noise, and shot noise, respectively. Note that the responsivity of the photodetector appears in the numerator and denominator. Therefore, its value does not need to be known in order to measure the output SNR. However, the photodetector quantum efficiency η appears in the shot noise term in the denominator because the number of detected photoelectrons differs from the number of photons that impinge on the photodetector. The noise figure is defined in terms of an ideal receiver, in which the quantum efficiency is unity. Thus when calculating the noise factor, it may be necessary to correct the measured SNR_{out} to account for nonunity quantum efficiency.

In general, the denominator of Eq. (8) depends on the optical frequency ν and the baseband frequency f. Rather than attempting to detail all of the individual frequency-dependent contributions to the denominator, we lump the noise terms in the denominator into the two noise categories: excess noise and shot noise [22]. Thus, the measured output SNR becomes

$$SNR_{\text{out}} = \frac{G^2 P_{\text{in}}^2}{B_e \left[S_e(\nu, f) + \eta^{-1} S_{\text{shot}} \right]}, \tag{9}$$

where the spectral density $S_e(\nu, f)$ includes all excess noise contributions to the output noise.

To obtain the amplifier noise factor as defined by Eq. (3), it is necessary to correct for source and receiver nonidealities, such as nonunity receiver quantum efficiency. When these nonidealities are corrected, the noise factor, according to Eqs. (3), (5), and (9), is:

$$\begin{aligned} F(\nu, f) &= \frac{S_e(\nu, f)}{2h\nu G^2 P_{\text{in}}} + \frac{S_{\text{shot}}}{2h\nu G^2 P_{\text{in}}} \\ F &= F_{\text{excess}} + F_{\text{shot}} \end{aligned} \tag{10}$$

$S_e(\nu, f)$ (units: W^2/Hz) is the overall amplifier-generated excess intensity noise density, $h\nu$ (units: joules) is the photon energy, G is the gain, and P_{in} (units: W) is the incident signal power [22]. The noise figure dependence on optical frequency,

ν, and baseband frequency, f, arises through the dependence of S_e on these variables. Equation (10) provides a basis for the measurement of F. The spectral density S_e is measured using electrical techniques at baseband frequencies, and if the other parameters are known or measured by standard optical measurements, the noise factor can be determined. This measurement method is referred to below as the *optoelectronic* or *electrical* method.

Next it will be shown that the standard optical noise factor used in the fiberoptic communications industry is a special case of Eq. (10) where all sources of SNR degradation are usually ignored except for signal-spontaneous beat and shot noise due to the received signal. This represents the best noise performance that a high gain amplifier can achieve when the input channel power is above the effective input noise of the amplifier for a given optical receiver bandwidth. For a typical 100 GHz ITU channel spacing with 10 GB/s transmission rates, the effective input noise ($\sim 2h\nu B_e$) is -50 dBm. This is well below the minimum channel powers used in these links.

As shown in Fig. 2, the well-known signal-spontaneous beat noise density depends on the product of the ASE density *in the same polarization state* as the signal and the amplified optical signal [3, 7]. At baseband frequencies below about 50 GHz the signal-spontaneous beat noise density is

$$S_{\text{sig-sp}} = 4\rho_{\text{ASE}} G P_{\text{in}}. \tag{11}$$

The shot-noise density due to the detected signal power P_{in} is

$$S_{\text{shot}} = 2h\nu G P_{\text{in}}. \tag{12}$$

Putting $S_e = S_{\text{sig-sp}}$ in Eq. (10), and substituting Eqs. (12) and (11), we obtain:

$$F = F_{\text{sig-sp}} + F_{\text{shot}}, \tag{13}$$

where

$$F_{\text{sig-sp}} = \frac{2\rho_{\text{ASE}}}{Gh\nu}$$

and

$$F_{\text{shot}} = \frac{1}{G}.$$

Equation (13) gives the noise factor for situations where signal-spontaneous beat noise and shot noise dominate. This noise factor can be measured using optical instrumentation. The ASE spectral density ρ_{ASE} can be measured using an optical spectrum analyzer. This approach to the measurement of the noise factor is referred to below as the *optical* method.

The IEC defines the signal-spontaneous noise factor as the first term in Eq. (13):

$$F_{\text{sig-sp}} = \frac{2\rho_{\text{ASE}}}{Gh\nu} \tag{14}$$

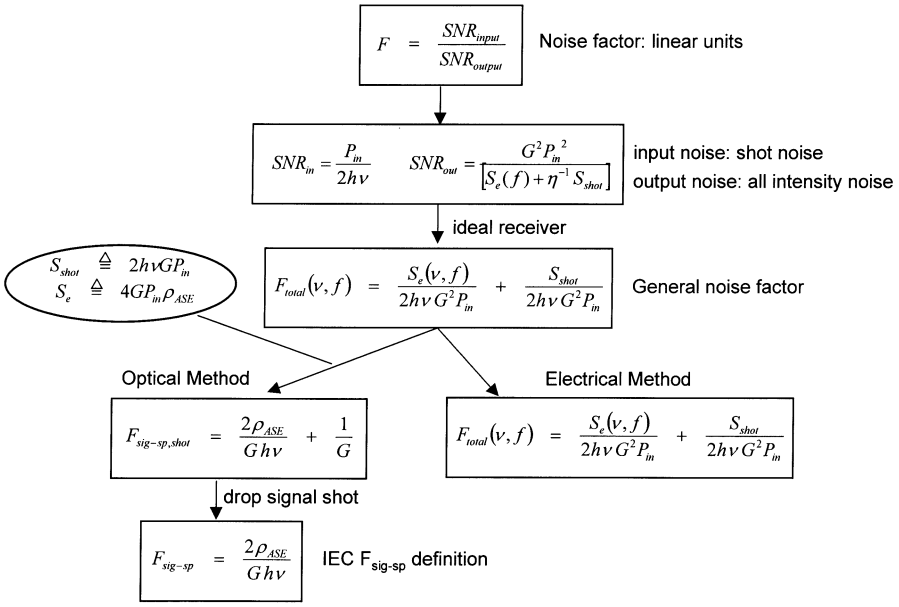

FIG. 6. The optical and electrical methods of optical noise figure measurement share the same general noise factor.

Figure 6 summarizes the development outlined above. Starting with the noise factor definition (see Eq. (3)), the specification of noise as intensity noise or equivalently photocurrent noise in an ideal receiver leads to the general noise factor (see Eq. (10)). This general noise factor is valid for either optical domain or electrical domain measurements of the noise factor. At this point, the path for optical measurements diverges from the path for electrical measurements. On the optical measurement path (to the left), the signal-spontaneous beat noise factor is easily characterized by measurement of the ASE density, ρ_{ASE}, and signal gain. Along the optoelectronic/electrical measurement path (to the right), the noise factor is measured using electrical measurements of S_e and S_{shot} as discussed in Section V. We note that a major advantage of the framework for noise factor presented in this paper is the common link of the general noise factor (Eq. (10)) both to optical and to optoelectronic/electrical characterization techniques for noise figure.

V. NOISE FACTOR OF CASCADED COMPONENTS

In this section we consider the noise factor of a cascade of optical components. The main objective of this section is to develop an expression for the total noise figure of a cascade of noisy components. This is an important consideration in a range of practical applications such as telecommunications links employing cascaded amplifiers.

In an amplifier cascade, the gain increases in a multiplicative fashion while the intensity noise increase depends on both multiplicative and additive processes,

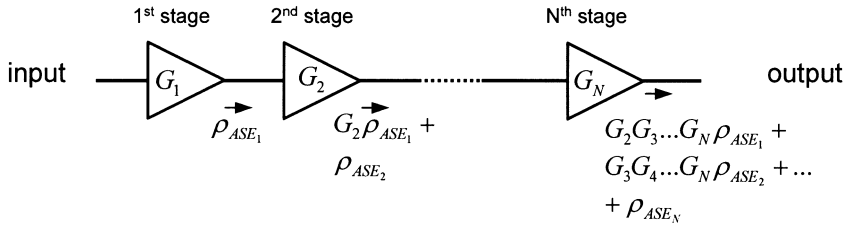

FIG. 7. Cascade of optical amplifiers leading to an accumulation of ASE.

depending on the characteristics of the particular noise source. Each stage of amplification adds additional noise to the signal as well as amplifying the noise generated from previous stages. This process is illustrated in Fig. 7, which shows a cascade of N amplifiers in which the ith stage has gain G_i and ASE spectral density ρ_{ASE_i}. The ASE from the first amplifier is multiplied by the gain of the second stage that in turn adds additional ASE. This process continues to the Nth amplifier stage. The ASE density ρ^c_{ASE} at the output of the cascade is

$$\rho^c_{\mathrm{ASE}} = \rho_{\mathrm{ASE}_1}(G_2G_3\ldots G_N) + \rho_{\mathrm{ASE}_2}(G_3G_4\ldots G_N) + \cdots + \rho_{\mathrm{ASE}_{N-1}}G_N + \rho_{\mathrm{ASE}_N}. \tag{15}$$

Given the gain, G, of each amplifier stage and the ASE contribution at each stage, the total ASE can be calculated. The signal-spontaneous noise factor $F_{\text{sig-sp}}$ for the amplifier is often used as a figure of merit indicating the amount of ASE generated by the amplifier per unit gain. With knowledge of the gain, G, and noise factor $F_{\text{sig-sp}}$, the total ASE density, ρ_{ASE} can be calculated. The noise figure of a cascade of amplifiers can then be determined in a straightforward manner as follows.

Dividing Eq. (15) by the total gain of the cascade, $G_{\mathrm{Total}} = G_1G_2\ldots G_N$, and multiplying by the quantity $(2/h\nu)$ gives the effective signal-spontaneous noise factor of the cascade:

$$\frac{2\rho^c_{\mathrm{ASE}}}{h\nu G_{\mathrm{Total}}} = \frac{2\rho_{\mathrm{ASE}_1}}{h\nu G_1} + \frac{2\rho_{\mathrm{ASE}_2}}{h\nu G_1G_2} + \cdots + \frac{2\rho_{\mathrm{ASE}_{N-1}}}{h\nu G_1G_2\ldots G_{N-1}} + \frac{2\rho_{\mathrm{ASE}_N}}{h\nu G_{\mathrm{Total}}}. \tag{16}$$

We find from Eqs. (14) and (16) that the total signal-spontaneous noise factor $F^c_{\text{sig-sp}}$ for a cascade of N stages of amplification is

$$F^c_{\text{sig-sp}} = F_{\text{sig-sp},1} + \frac{F_{\text{sig-sp},2}}{G_1} + \frac{F_{\text{sig-sp},3}}{G_1G_2} + \cdots + \frac{F_{\text{sig-sp},N}}{G_1\ldots G_{N-1}}, \tag{17}$$

where $F_{\text{sig-sp},N}$ is the noise factor of the Nth stage. The same amplifier cascade relation is given by Desurvire [1] and Agrawal [5] and has also been shown to be applicable for coherent detection [23].

If the signal-spontaneous noise factor, $F_{\text{sig-sp}}$, is measured for each amplifier in the cascade, the cascade noise factor, $F^c_{\text{sig-sp}}$, is calculated from Eq. (17) and the expected ASE density at the end of the chain of amplifiers from Eqs. (16) and

(17) is

$$\rho^c_{\text{ASE}} = F^c_{\text{sig-sp}} \frac{h\nu}{2} G_{\text{Total}}. \tag{18}$$

This ASE density, ρ^c_{ASE}, is strictly in the same polarization as the signal light. The total unpolarized ASE is twice the polarized ASE if the effects of polarization hole-burning (PHB) or polarization-dependent loss may be neglected [3]. In large amplifier cascades, however, PHB may become significant.

Once the cascade signal-spontaneous noise factor, $F_{\text{sig-sp}}$, is determined, shot noise can be included according to Eq. (13) (with $\eta = 1$) to compute the overall signal-spontaneous and shot-noise-limited noise factor $F^c_{\text{sig-sp, shot}}$ of the cascade of N stages:

$$F^c_{\text{sig-sp, shot}} = F^c_{\text{sig-sp}} + \frac{1}{G_1 G_2 \ldots G_N}. \tag{19}$$

EXAMPLE: NOISE FACTOR OF THREE ELEMENT CASCADE. We now illustrate the cascade formulas of the three-element cascade of two amplifiers and a passive element shown in Fig. 8. The passive element may be some device such as an optical wavelength add/drop multiplexer or a chromatic dispersion compensator.

To determine the overall noise factor, we first determine the signal-spontaneous noise factor $F^c_{\text{sig-sp}}$ for a cascade of three elements using Eq. (17):

$$F^c_{\text{sig-sp}} = F_{\text{sig-sp, 1}} + \frac{F_{\text{sig-sp, 2}}}{G_1} + \frac{F_{\text{sig-sp, 3}}}{G_1 G_2}. \tag{20}$$

As shown in Fig. 8 we set G_2 to L, the transmission coefficient of the passive element ($L \leq 1$). The ASE and hence the excess noise factor contributed by the passive element are zero, and we obtain:

$$F^c_{\text{sig-sp}} = F_{\text{sig-sp, 1}} + \frac{0}{G_1} + \frac{F_{\text{sig-sp, 3}}}{G_1 L}. \tag{21}$$

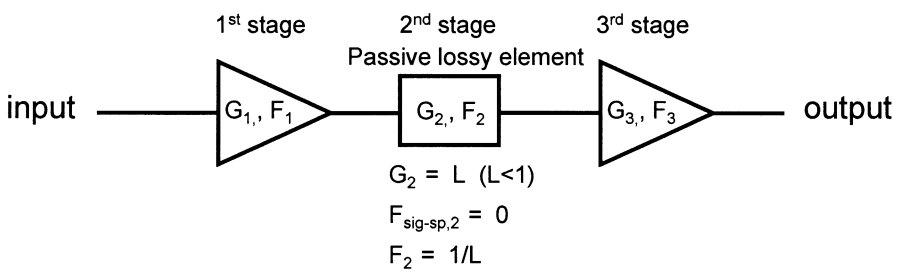

FIG. 8. Cascade of optical amplifiers and a passive element.

The noise factor including shot noise from Eq. (19) is:

$$F^{c}_{\text{sig-sp, shot}} = F_{\text{sig-sp, 1}} + \frac{F_{\text{sig-sp, 3}}}{G_1 L} + \frac{1}{G_1 L}. \tag{22}$$

From this we conclude that if $G_1 L$ is less than unity, then both the first and the third devices must have low noise figures to minimize the overall noise figure. As the product $G_1 L$ exceeds unity, the first amplifier dominates the overall noise contribution. It is worth noting that with the noise figure formulations derived here, the noise factor of a passive lossy device is equal to its loss. A 10 dB attenuator has a noise figure of 10 dB.

Discussion

The noise figure formulation presented in Eq. (10) is the main result of our theory discussion. It provides a consistent and rigorous basis for dealing with the total noise figure where effects such as multipath interference noise are taken into account. The formulation presented here provides a common model between optical and electronic measurement methods allowing for measurement of the complete noise figure.

We have also presented a reduced formulation when only signal-spontaneous beat noise and shot noise need to be included in the model. The reduced formulation (summarized in Eq. (13)) is useful for evaluating the effects of gain and loss on the noise characteristics of cascades of optical components. However, it is important to note that this reduced formulation is strictly applicable only where signal-spontaneous beat noise and shot noise are the only noise of interest. The reduced formulations described above are in agreement with both the IEC (SC86C, Working Group 3) draft document concerning optical amplifier noise figure and the instrumentation offered by suppliers of noise figure test equipment.

VI. MEASUREMENT OF NOISE FIGURE

Noise figure has been traditionally characterized using the so-called optical and optoelectronic or electrical techniques [3, 12, 15–23]. In the optical techniques, an optical spectrum analyzer is used to measure the amplified spontaneous emission from which the noise factor is found using Eq. (13). In the optoelectronic/electrical method, a photodetector followed by an electrical spectrum analyzer is used to directly measure the intensity noise from which the noise figure is determined. The optoelectronic/electrical method reveals the baseband frequency dependence of the amplifier noise figure.

In both measurement methods, it is important to refer the amplifier noise performance to a defined set of terminals. This was illustrated earlier in Fig. 5, which shows how noise figure is measured. In Fig. 5a the input and output reference planes are connected by a lossless waveguide (fiber). In Fig. 5b the amplifier is inserted between the reference planes. Input power is defined by the IEC as the power exiting the input connector, or cleaved fiber (prior to the fusion

splice connection). To reduce the additive effects of broadband SSE power on the input power to the EDFA, the laser source(s) should be postfiltered. Polarization randomizers are often used to reduce measurement uncertainty caused by slowly wondering light polarization and polarization dependent elements in the test system.

The input coupling loss can have a dramatic effect on the measured noise figure. This is illustrated by an experience one of the authors had while participating in a series of optical amplifier noise figure measurement seminars. A manufacturer of optical amplifiers brought their amplifier to the HP automated noise figure measurement system traveling with the seminar. Upon testing, the measured noise figure was over 10 dB. The manufacturer's amplifier experts insisted that the noise figure was closer to 6 dB. After some investigation it was found that a dirty amplifier input connector was the culprit. After cleaning, the amplifier performed as expected. The effect of input coupling loss can be readily determined by using the cascade formula Eq. (20) or by using Eq. (10). If the input coupling loss is an amplifier defect, then it will increase the noise figure. If, instead, it is a test system defect, it must be corrected. For the most accurate measurements, fusion spliced connections are preferred. At a minimum, given the impact of the input connector losses and potential input mode mismatch, the pertinent connector details should be recorded along with the measured noise figure data.

Optical Measurement Techniques

From Eq. (13), measurement of the optical noise figure requires the following parameters to be determined:

- The ASE spectral density ρ_{ASE} in the signal polarization at the channel wavelength
- The channel wavelength
- The device gain G.

The ASE spectral density is easily measured using an optical spectrum analyzer (OSA). The gain and wavelength can be measured using a variety of conventional techniques.

The recent evolution of dense wavelength division multiplexing (DWDM) with its narrow spacing of signal channels has increased the need for careful attention to separation of the laser source spontaneous emission (SSE) from ASE generated in the device under test. Laser source spontaneous emission is the amplified spontaneous emission produced by the internal optical gain of the laser transmitter. It is very similar to the ASE produced by optical amplifiers. It is clearly important that any nonideal source characteristics do not influence the accuracy of the measurement. The maximum acceptable SSE to obtain a reasonable error in the measured noise figure depends on the absolute SSE density at the amplifier terminals. Figure 9 shows the fractional error in the measured noise factor as a function of the SSE. We see that a source with -50 dBm/nm SSE spectral density at the signal wavelength would add 50% to the measured noise factor. For this

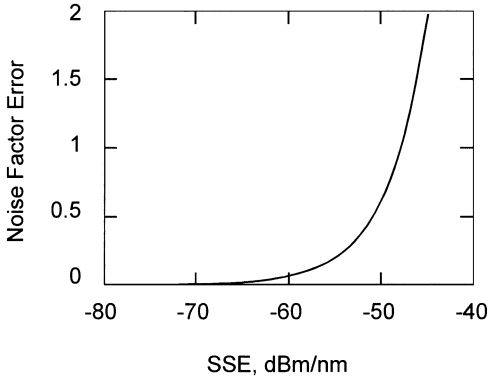

FIG. 9. Noise factor error due to additive effect of source spontaneous emission (SSE) on noise figure.

particular optical source, a reduction of better than 15 dB in the SSE is required for accurate measurement. This reduction could be performed by attenuating the test source or by using the techniques outlined below.

A number of refinements of the optical method have been developed for accurate noise figure characterization including:

- Source subtraction
- Time domain extinction
- Polarization extinction
- Reduced source
- Signal substitution.

In all these measurements, the amplifier gain is measured at the signal wavelengths and the amplifier generated ASE is measured preferably at the same wavelength or estimated through wavelength interpolation. Note that all the techniques described here require accurate information regarding the effective noise bandwidth of the OSA. The nominal measurement resolution bandwidth is not necessarily equal to the effective optical noise bandwidth. Moreover, the effective noise bandwidth typically varies with optical wavelength. Fortunately, manufacturers typically supply the wavelength dependent effective noise bandwidths of their OSAs.

Source Subtraction Technique

The source subtraction technique addresses the problem of separating the SSE from the ASE by characterizing the SSE with the EDFA bypassed [3]. As long as the SSE spectral density is time-invariant, in principle it may be subtracted from the total noise output of the EDFA to obtain the EDFA-generated ASE. Equation (13) is modified to accommodate the subtraction yielding:

$$F = \frac{2\rho_{\text{total}}}{Gh\nu} + \frac{1}{G} - \frac{2\rho_{\text{SSE}}}{h\nu}. \tag{23}$$

noise factor = measured noise factor − SSE correction

In Eq. (23), ρ_{total} is the total ASE density from the optical amplifier including the amplified source spontaneous emission, both in the same polarization state as the signal. In practice, the ASE is usually assumed to be unpolarized and the densities $2\rho_{\text{total}}$ and $2\rho_{\text{SSE}}$ are replaced by their corresponding unpolarized densities. Since the presence of the signal masks the measurement of the noise densities at the signal wavelength, measurements adjacent to the signal are used to interpolate the noise at the signal wavelength as shown in Fig. 10. In the figure, the input signal spectrum clearly shows significant SSE.

This technique is applicable to multichannel characterization of EDFAs under certain restrictions. It requires an OSA with sufficient selectivity to measure between closely spaced DDM channels. The effect of cumulative SSE needs to be considered. In particular, if the DWDM test lasers are combined using broadband fused couplers, the broadband SSE from all channels will be additive at each measurement wavelength. This can result in the subtraction of two noise measurements of similar magnitude, thus increasing the error in the correction. Limiting the total amplified SSE density to be less than or equal to the ASE density generated by an ideal amplifier with a 3 dB noise figure, we find that the composite SSE power would preferably be less than $2h\nu B_o$. At a wavelength of 1.55 μm, this corresponds to a maximum composite SSE density of ~ -45 dBm/nm at the EDFA input terminals.

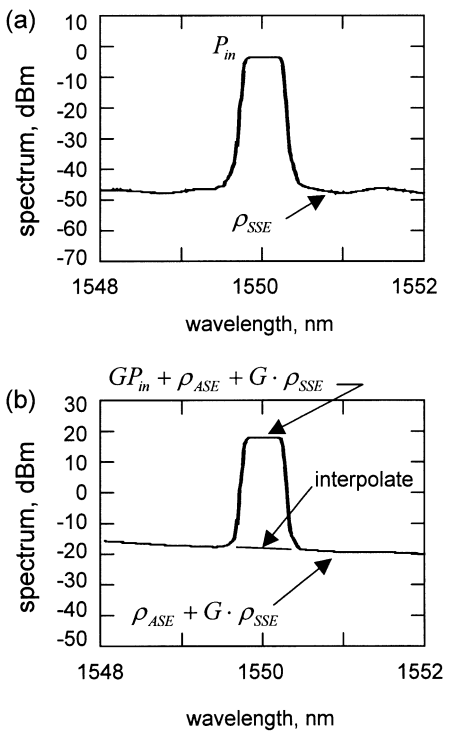

FIG. 10. Optical spectra for source subtraction method of noise figure measurement: (a) incident signal and SSE, (b) output spectrum.

Time Domain Extinction Technique

The time domain extinction (TDE) method takes advantage of the slow gain dynamics of the EDFA to reduce the effect of SSE on the noise figure measurement [3, 18, 19, 24]. When the EDFA is driven into saturation, the gain and the ASE depend on the average incident signal intensity. When the signal is pulsed-off, the EDFA gain recovers to a new steady state level. The recovery time is slow enough (microsecond time-scales) such that the ASE from the amplifier may be measured before it changes appreciably. Since the signal and SSE are no longer present, the measured ASE corresponds to the actual ASE generated by the optical amplifier. The signal is then pulsed back on and the process repeats.

A measurement setup for this technique is shown in Fig. 11. When the input switch is closed as shown in Fig. 11a, the amplifier is illuminated by signal and noise. In Fig. 11b, the input switch is opened extinguishing the signal and the output switch closes. This enables the OSA to sample the ASE produced by the amplifier. When the gating rate is slow compared to the gain recovery time of the amplifier, the response is as shown in Fig. 12a. Energy storage in the amplifier causes a signal transient as the signal is gated into the amplifier operating in the small signal regime [1, 3]. The flat portion of the waveform following the transient is the steady state condition. If the ASE is measured soon after the signal is gated off, it will be the same ASE generated in the presence of signals. When the gating rate is faster than the gain recovery time of the amplifier, the response is as shown in Fig. 12b. In this case the effective input power that determines the amplifier saturation state is the time average of the gated signal. The ASE waveform is triangular with an offset during the signal-on interval due to the additive effect of the SSE. If the ASE is sampled halfway through the positive going slope as shown, the ASE will correspond to the ASE generated by the amplifier in the presence of the average signal power. The error due to gain recovery varies linearly with pump power [3]. For EDFAs, pulse repetition rates of 25 kHz or more are typically used.

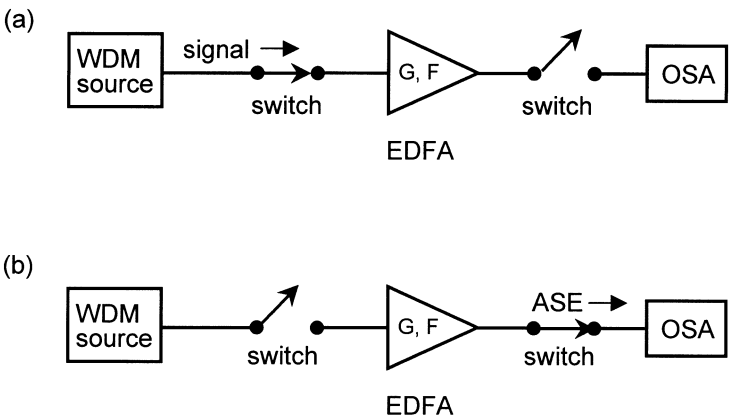

FIG. 11. Time-domain extinction method for amplifier ASE measurement. (a) Signal is setting amplifier saturation state. (b) Signal disconnected, OSA measures ASE.

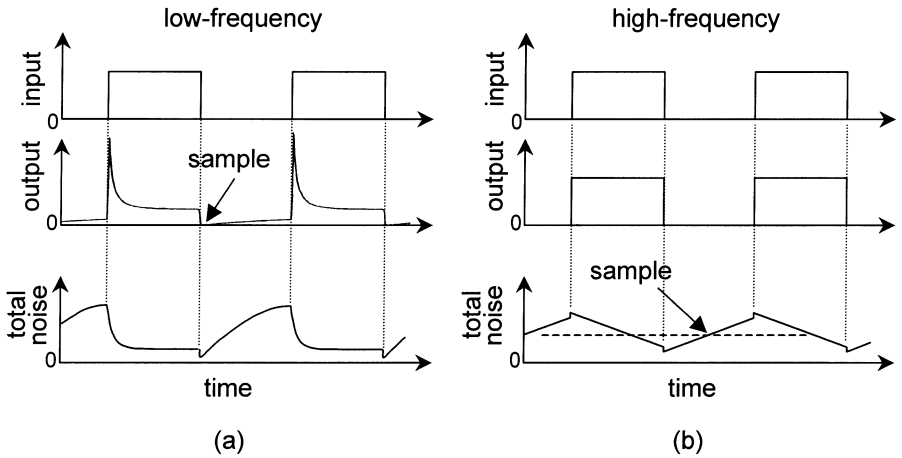

FIG. 12. Signal and ASE diagrams for domain extinction method for amplifier. (a) Low frequency regime. (b) High frequency regime.

The presence of active feedback and control circuits will also affect the choice of the signal gate-rate.

The extinction ratio of the switches shown in Fig. 11 is important. Multiple switch stages may be required to obtain complete suppression of the signal. When the depth of the extinction is not sufficient to completely reject the signal, interpolation is used to estimate the ASE at the signal wavelength.

With the addition of a small signal probe, a swept-wavelength characterization of the EDFA gain spectrum can be performed [3, 25]. This permits gain tilt characterization for DWDM applications by measuring the variation in gain between the test laser wavelengths. Figure 13 shows a typical measurement of gain and noise figure using this technique. In Fig. 13a, the pulsed edge-emitting LED (EELED) probe provides a broadband stimulus from a wavelength of 1525 to 1575 nm. Three measurements are performed during the time interval when the saturating source is gated off:

1. Calibration: small-signal probe power versus wavelength with EDFA bypassed: $P_{\text{cal}}(\lambda)$

2. Small-signal probe power and ASE power versus wavelength with EDFA inserted: $P_1(\lambda)$

3. ASE power versus wavelength with EDFA inserted (probe not sampled): $P_2(\lambda)$

The amplifier gain is calculated using:

$$G(\lambda) = \frac{P_1(\lambda) - P_2(\lambda)}{P_{\text{cal}}(\lambda)}. \tag{24}$$

Figure 13b shows a measured noise figure using this technique. The noise factor was calculated using Eq. (13) with $\rho_{ASE}(\lambda) = P_2(\lambda)/(2B_o)$, where B_o is the effective noise bandwidth of the OSA.

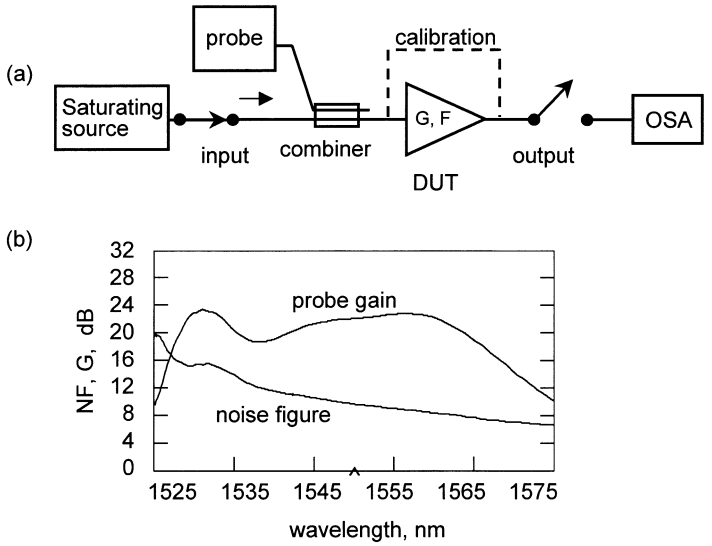

FIG. 13. (a) Dynamic gain and noise figure measurement setup. (b) Measurement with a saturation wavelength of 1550 nm.

Polarization Extinction Technique

The polarization extinction technique provides another way to deal with the problem of excess source noise [3, 18]. In this method, a fixed, or known, relationship is assumed to exist between the magnitude of the ASE generated by the optical amplifier in orthogonal polarizations. Therefore, if the ASE is measured in one polarization, the ASE in the signal polarization is determined. In the measurement setup shown in Fig. 14, a polarized signal source is directed to the optical amplifier. To measure the ASE, the polarization controller following the amplifier is set such that the signal polarization is orthogonal to the preferred transmission axis of the polarizer. Under these conditions, the signal, the amplified SSE, and one-half the ASE are reflected away. The OSA measures only the ASE orthogonal to the signal. Noise factor is calculated from Eq. (13) where the ASE densities are assumed equal in each polarization.

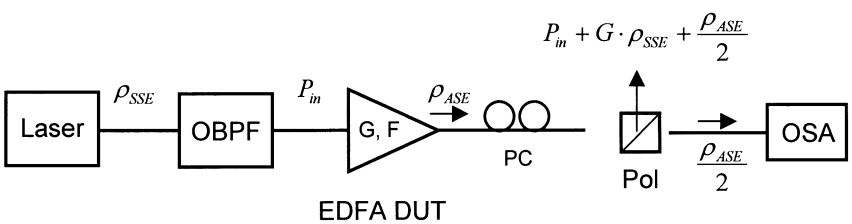

FIG. 14. Polarization extinction method for amplifier noise figure measurement. Laser has polarized output. OBPF, optical bandpass filter; PC, polarization controller; Pol, polarizing beam splitter; OSA, optical spectrum analyzer.

In practice, the rejection of the signal may not always be complete. The signal may still contribute to the displayed spectrum. Even so it will be adequate to sufficiently reduce the noise figure error. As with the TDE technique, when the depth of the null is not sufficient as determined from Fig. 9, interpolation is used to estimate the ASE at the signal wavelength.

Factors limiting the SSE rejection include:

- The time required to adjust the polarization controller to obtain the desired null depth
- Polarization mode dispersion
- The stability of test system birefringence (test cable stability)
- The quality of polarizer rejection
- SSE from other DWDM channels

The amplifier gain is measured by bypassing the polarizer and performing the gain measurement in the conventional manner. Beyond the necessary rejection of the signal ASE, there is an added benefit with this technique of allowing measurement closer to the signal wavelength. The limited wavelength selectivity of an OSA means that the ability to measure low levels of ASE decreases as the OSA is tuned close to the strong test channel. The 25 dB, or more, rejection of the signal that this technique provides allows for a close-in measurement of the ASE around the optical signal. An example of a rejected signal (amplifier bypassed) and the case where the polarization controller is set to maximize the signal is shown in Fig. 15 [3].

Signal-Substitution Technique

The signal-substitution technique allows for measurement of the ASE at the channel wavelength by removing the signal and adding power to adjacent channels [26]. This technique reduces the wavelength selectivity requirement on the OSA for a given channel spacing. This allows for measurement on dense DWDM channel plans. The method is based on the locally homogeneous nature of the optical amplifier gain spectrum. The concept is illustrated in Fig. 16. The signal power at

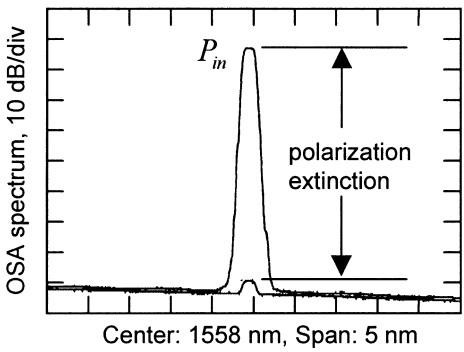

FIG. 15. Input signal and laser spontaneous emission rejection using polarization extinction.

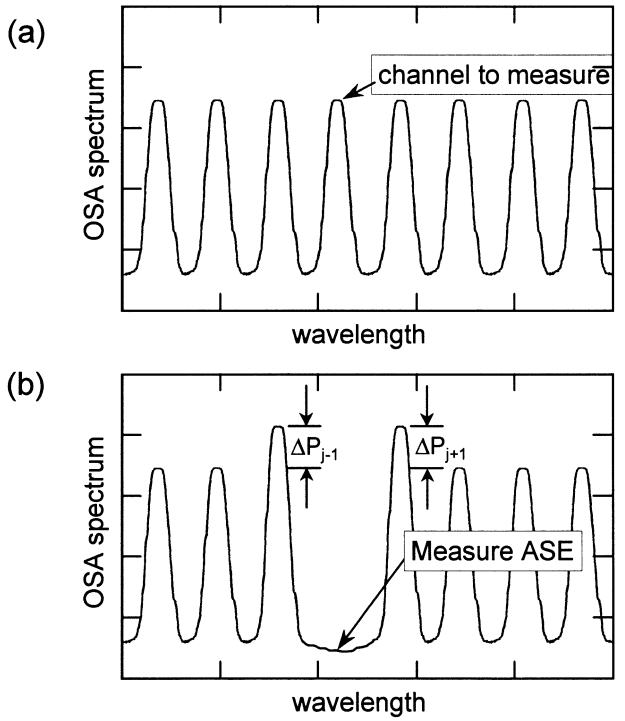

FIG. 16. Illustration of the signal substitution technique: (a) input DWDM channels, (b) signal at test channel is displaced to adjacent channels.

the channel wavelength to be characterized is removed. The removed signal power that had contributed to the local and global amplifier saturation state is accounted for by increasing the power of the adjacent channels. For closely spaced channels, ΔP, the required increase in adjacent channel powers is given by

$$\Delta P_{i-1}, \Delta P_{i+1} = \frac{P_i G_i}{G_{i-1} + G_{i+1}}, \tag{25}$$

where P_i and G_i are the power and gain of the test channel, respectively. The noise figure measurements are performed in combination with the source subtraction method to reduce the impact of the source spontaneous emission. Since the method provides constant input power to the EDFA during the measurement, it does not interact with optical power control feedback circuits employed with most EDFAs.

DWDM Characterization: Reduced Channel Technique

In dense WDM application with a large number of input channels, the cost of assembling and maintaining a large number of stable test-quality sources provides motivation to reduce the required DWDM laser array. In these applications the

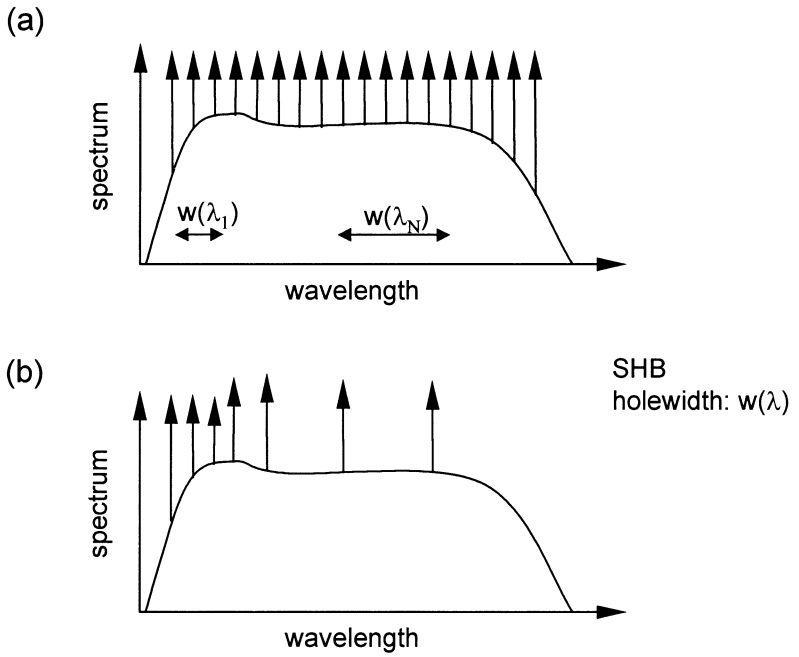

FIG. 17. Illustration of the amplifier spectrums for the reduced-source technique. (a) DWDM channel plan. (b) Equivalent reduced-source representation. SHB, spectral hole-burning.

reduced-channel technique may be applied [27]. The underlying premise is that the EDFA behaves like a homogeneously broadened amplifier across a limited wavelength range. The EDFA, across its entire gain band, has significant homogeneous broadening. That is, all the signals across the EDFA gain band can equally access the stored energy responsible for gain anywhere across the band. However, measurements have revealed the presence of spectral hole-burning (SHB) with a dependency of ~ 0.3 dB for each dB of gain compression [1, 3, 29]. Thus the accuracy of a method that uses a single high-power channel to represent the ensemble of DWDM channels would be limited by SHB. In general, in the presence of SHB, N channels are used to represent M actual channels ($N \leq M$) across the wavelength range of the channel plan. The separation of the N channels is determined by the widths of the spectral holes. For example, a minimum of one channel per SHB hole-width should be used. Spectral hole widths vary from about 3 nm to greater than 10 nm across the EDFA gain region. The narrower holes tend to be around the 1530 nm region which implies more saturating channels to cover this region. The reduced-source concept is shown in Fig. 17. In Fig. 17a, the actual test channel plan is illustrated along with the SHB holewidth. A possible set of representative channels is indicated in Fig. 17b.

In physical terms, the representative powers applied to the amplifier must ensure that the amplifier state, as set by the relative levels of the metastable-state and ground-state populations, is the same for the complete channel and the reduced channel technique. The representative power, P_{rep} for a set of q wavelengths is

equal to [27]:

$$P_{\text{rep}} = \frac{1}{\lambda_{\text{rep}} G_{\text{rep}}} \sum_q P_q \lambda_q G_q. \tag{26}$$

This is another way of saying that the reduced channel representation across a given homogeneously broadened portion of the gain spectrum must generate the same corresponding photon flux as that generated by the full complement of channels across the same portion of the gain spectrum. In this technique, the various channel gains are not known in advance, so they can be set equal to G_{rep} as a starting guess. Measurements using this technique have shown rapid convergence, typically in about two iterations [27].

Optoelectronic / Electrical Measurement Techniques

The most complete evaluation of noise in an amplifier or other optical component is performed using a photodetector and an electrical spectrum analyzer (ESA) to examine the intensity noise generated by the optical amplifier [3, 9, 12, 15, 22, 28]. The optoelectronic/electrical measurement method has a major advantage over optical methods. Unlike optical methods, all amplifier-generated intensity noise that would occur in an actual receiver such as multipath interference noise, double Rayleigh scattering, and pump-induced noise are measured by this technique. Optoelectronic methods therefore provide the only means to completely characterize the intensity noise generated by an optical amplifier.

A measurement setup for the optoelectronic technique is shown in Fig. 18. Optical filters following the source and preceding the detection are shown to indicate that the source linewidth and receiver optical bandwidth are test parameters that must be specified. This is due to the optical bandwidth dependence of various noise processes such as interference noise and spontaneous-spontaneous beat noise.

The general noise factor relation (Eq. (10)) applicable to both optical and optoelectronic methods provides the starting basis for the optoelectronic method.

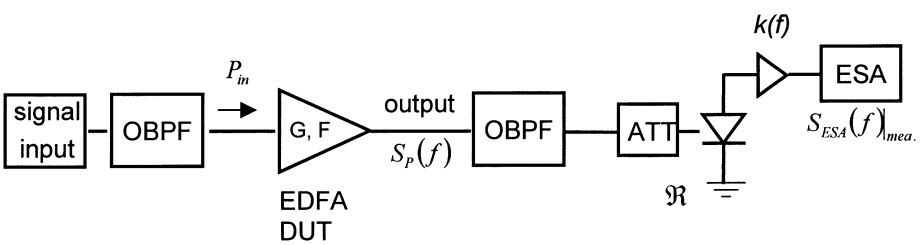

FIG. 18. Noise figure measurement using an electrical spectrum analyzer (ESA). OBPF, optical bandpass filter; ATT, optical attenuator.

For an ideal receiver, with $\eta = 1$, the total noise factor is as given in Eq. (10), repeated here for convenience,

$$F_{\text{total}}(\nu, f) = \frac{S_e(\nu, f)}{2h\nu G^2 P_{\text{in}}} + \frac{S_{\text{shot}}}{2h\nu G^2 P_{\text{in}}},$$

$$F_{\text{total}} = F_{\text{excess}} + F_{\text{shot}} \tag{27}$$

where $S_e(\nu, f)$ is the amplifier-generated excess intensity noise and S_{shot} is the shot noise due to the total average power exiting the amplifier. The dependence of the noise figure on baseband frequency f is of particular importance with optoelectronic techniques. There are several approaches to making this measurement as discussed in [12, 15, 17, 22]. More detail on the discussion given here may also be found in [3].

The net noise power density displayed on the ESA with the setup shown in Fig. 18 consists of contributions from the excess amplifier noise, $S_e(f)|_{\text{EDFA}}$, the amplified excess source noise, $S_e(f)|_{\text{source}}$, the shot noise, $S_i|_{\text{shot}}$, and the thermal noise, $S_{\text{ESA}}(f)|_{\text{th}}$:

$$S_{\text{ESA}}(f)|_{\text{mea}} = |k(f)|^2 \left[\Re^2 S_e(f)\big|_{\text{EDFA}} + \Re^2 G^2 S_e(f)\big|_{\text{source}} + S_i|_{\text{shot}} \right] + S_{\text{ESA}}(f)|_{\text{th}} \ [\text{W/Hz}]. \tag{28}$$

$|k(f)^2|$ is nominally 50 Ω, but it must be calibrated across the measurement frequency range. Electrical preamplifier limitations, impedance mismatches, and the frequency response of the ESA and photodetector will cause $|k(f)^2|$ to vary with baseband frequency. $\Re$ is the DC responsivity of the photodetector with units of [A/W]. G is the gain of the optical amplifier. In the following, we assume that the amplifier gain and the optoelectronic detection calibration has been determined using standard methods as described in [3]. The test method must extract the excess intensity noise $S_e(f)|_{\text{EDFA}}$ generated by the EDFA from the measurement system characteristic and the source and receiver excess noises. Once this is performed the noise factor can be calculated using Eq. (27).

Source Noise Subtraction Technique:

With this method a first measurement is made with the EDFA bypassed to determine the level of excess noise from the source. The first ESA measurement yields:

$$S_{\text{ESA}}(f)|_{\text{mea. \#1}} = |k(f)|^2 \left[\Re^2 S_e(f)\big|_{\text{source}} + 2q\Re\langle P_{\text{in}} \rangle \right] + S_{\text{ESA}}(f)|_{\text{th}}. \tag{29}$$

$|k(f)^2|$ and $\Re$ are known from the system calibration, the input power, P_{in}, is measured using an optical power meter, and the thermal noise is determined by blocking the input light and recording the ESA displayed noise. Thus the excess source noise $S_e(f)|_{\text{source}}$ is characterized.

Next the EDFA is inserted and a second measurement is made with the calibrated attenuation, α, set such that the receiver does not saturate:

$$S_{\mathrm{ESA}}(f)|_{\mathrm{mea.\,\#2}} = |k(f)|^2\left[\Re^2\alpha^2 S_e(f)|_{\mathrm{EDFA}} + \Re^2\alpha^2 G^2 S_e(f)|_{\mathrm{source}} + 2q\Re\,\alpha\langle P_{\mathrm{ave}}\rangle\right] + S_{\mathrm{ESA}}(f)|_{\mathrm{th}}. \quad (30)$$

The average incident power $\langle P_{\mathrm{ave}}\rangle$ including both amplified signal and ASE is measured with an optical power meter. This results in one equation and one unknown (the amplifier excess noise) with the solution:

$$S_e(f)|_{\mathrm{EDFA}} = \frac{S_{\mathrm{ESA}}(f)|_{\mathrm{mea.\,\#2}} - S_{\mathrm{ESA}}(f)|_{\mathrm{th}}}{|k(f)|^2\Re^2\alpha^2} - \frac{2q\langle P_{\mathrm{ave}}\rangle}{\Re\,\alpha} - G^2 S_e(f). \quad (31)$$

$$\textit{Amplifier noise} = \left[(\textit{ESA noise} - \textit{thermal noise})/\textit{receiver correction}\right] - \textit{shot noise} - \textit{amplified source excess noise}$$

With the excess amplifier noise known, the noise figure is calculated according to Eq. (27).

Constant Power Technique

With this method, a first measurement is made with the EDFA bypassed and the input attenuator is set for unity transmission (e.g., $\alpha = 1$) [15]. A spectral measurement with the ESA yields:

$$S_{\mathrm{ESA}}(f)|_{\mathrm{mea.\,\#1}} = |k(f)|^2\left[\Re^2 S_e(f)|_{\mathrm{source}} + 2q\Re\langle P_{\mathrm{in}}\rangle\right] + S_{\mathrm{ESA}}(f)|_{\mathrm{th}}. \quad (32)$$

The amplifier is inserted and the attenuation is increased ($\alpha < 1$) such that the average power is the same as in the first measurement. If the amplified signal and ASE are the only powers present at the detection, the attenuation would equal

$$\alpha = \frac{\langle P_{\mathrm{in}}\rangle}{\langle GP_{\mathrm{in}}\rangle + \langle P_{\mathrm{ASE}}\rangle} \quad (33)$$

and the displayed spectrum is

$$S_{\mathrm{ESA}}(f)|_{\mathrm{mea.\,\#2}} = |k(f)|^2\left[\Re^2\alpha^2 S_e(f)|_{\mathrm{EDFA}} + \Re^2\alpha^2 G^2 S_e(f)|_{\mathrm{source}} + 2q\Re\,\alpha\left[\langle GP_{\mathrm{in}}\rangle + \langle P_{\mathrm{ASE}}\rangle\right]\right] + S_{\mathrm{ESA}}(f)|_{\mathrm{th}} \quad (34)$$

with the constraint that the signal and ASE satisfy

$$\langle GP_{\mathrm{in}}\rangle \gg \langle P_{\mathrm{ASE}}\rangle. \quad (35)$$

Then subtracting Eq. (32) from Eq. (34) yields:

$$S_{\mathrm{ESA}}(f)|_{\mathrm{mea.\#2}} = |k(f)|^2 \Re^2 \alpha^2 S_e(f)|_{\mathrm{EDFA}}. \tag{36}$$

$S_e(f)|_{\mathrm{EDFA}}$ is then determined by using the measured receiver transfer function.

In practice, it is advisable to use a low-noise optical receiver with a high saturation power preceding the electrical spectrum analyzer. This is particularly important where high channel powers require optical attenuation preceding the receiver to limit saturation. Optical attenuation reduces the detected intensity noise relative to the thermal and shot noise making it desirable to use a receiver which can sustain high optical power levels.

Impact of Source Linewidth and Receiver Bandwidth

In a system otherwise free of optical reflections, internal reflections within the optical amplifier convert signal phase and frequency noise into intensity noise [3, 8, 9, 11]. The amount of intensity noise depends equally on the strength of the reflections and on the laser linewidth. Thus the signal linewidth becomes a stimulus parameter, much like optical power or signal wavelength. It can be argued that an ideal amplifier has no MPI and thus the conversion of phase noise to intensity noise through amplifier MPI is an amplifier nonideality which should be included in the amplifier noise figure. Certainly, this increase in intensity noise manifests itself as increased bit-error rates at the destination communications receiver. Therefore, the source phase noise, or, in practical terms, its linewidth, should be noted as a source parameter. The receiver bandwidth, B_o, also determines the contribution spontaneous-spontaneous beat noise will make to the noise figure as suggested in Fig. 3. This bandwidth may be set by the filter shape of a DWDM demultiplexer or by the net lineshape of the atomic transitions responsible for the amplifier gain. In any case, this should be specified when spontaneous-spontaneous beat noise is expected to contribute to the noise figure.

Example RIN Transfer Technique of Optoelectronic Noise Figure Measurement

The noise figure of a 980 nm copropagating amplifier with integrated tap unit was measured using the optoelectronic method with the RIN transfer noise calibration method. The amplifier gain was measured to be 35. First, the opto-electronic receiver was calibrated using the RIN transfer technique [3]. A dielectric thin film filter of approximately 433 GHz FWHM was placed after an EDFA to provide a calibration noise source. The spectrum, $S_E(\nu)$, of the noise source was measured with an OSA. The expected RIN for the ASE source was calculated according to [3],

$$RIN_{\mathrm{cal}}(f) = \frac{FT\left[\left|FT^{-1}\{S_E(\nu)\}\right|^2\right]}{\left[\int S_E(\nu)\, d\nu\right]^2}, \tag{37}$$

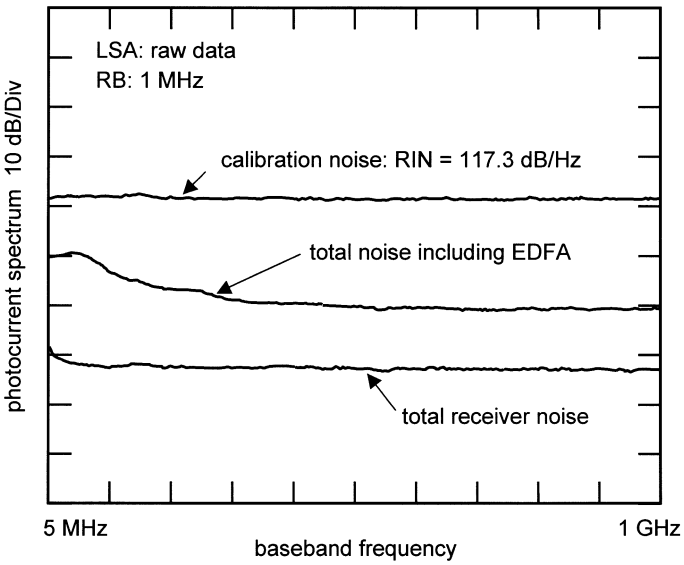

FIG. 19. Data from electrical-method noise figure measurement showing calibration, amplifier total, and receiver noise traces. Dependence of EDFA noise figure on baseband frequency is shown in the middle trace.

which yielded a RIN of -117.3 dB/Hz for the calibration source. This source was then measured using a photodetector electrical spectrum analyzer combination as shown by the top trace in Fig. 19. The average power of the ASE source was 1.342 mW. With this information and the following definition of RIN,

$$RIN_{\text{cal}}(f) = \frac{S_e(f)}{P^2}, \tag{38}$$

the absolue magnitude of the electrical spectrum analyzer display was calibrated with units of W/Hz plotted on a logarithmic scale.

Next, the thermal noise was measured with the input light to the receiver blocked as shown by the lower trace in Fig. 19. In the next step, the DUT EDFA was connected and illuminated with a semiconductor DFB laser with -18.2 dBm of shot-noise-limited output at a wavelength of 1558.8 nm. The corresponding noise trace is shown in Fig. 19. Note that at frequencies below 500 MHz there is an increase in the EDFA noise. This is due to optical reflections internal to the amplifier causing an MPI-induced noise increase. Using Eq. (28), the noise figure at 300 MHz was 7.8 dB, rising to about 16 dB at low frequencies. Near 1 GHz, the noise figure dropped by approximately 2 dB. This is in contrast to a noise figure of 5.8 dB as measured using the optical method and Eq. (13). The difference is due to amplifier-generated intensity noise that the opto-electronic method measures which is neglected with the optical test methods.

At a risk of over-generalizing, and adding the cautionary note that the basic techniques discussed below will evolved over time, we summarize below the merits and disadvantages of the various optical and optoelectronic/electrical measurement methods.

Optical Methods

Time domain extinction. Merits: Provides rapid measurement. Can be used in conjunction with small-signal probe to measure dynamic gain. Works well with the reduced-source technique. Allows possibility for noise measurement at the signal wavelength. Disadvantages: Insertion loss of gating switches, more complicated measurement setup.

Source subtraction. Merits: Simple to implement. Disadvantages: sensitive to additive SSE from DWDM channels, requires stable SSE.

Polarization extinction. Merits: Allows possibility for noise measurement at the signal wavelength. Disadvantages: longer measurement time, sensitive to polarization mode dispersion, polarization stability and polarization hole-burning.

Signal substitution. Merits: Reduces wavelength resolution requirement of the OSA, maintains constant power to the EDFA, simple to implement. Disadvantages: sensitive to spectral hole-burning in certain applications.

Reduced-source. Merits: Reduces size of DWDM test laser array. Disadvantages: iterative method (~ 2 iterations), largest benefit obtained where the SHB widths are wider than DWDM channel separations.

Optoelectronic / Electrical Methods:

RIN transfer technique. Merits: Provides complete noise figure with baseband frequency dependence of noise factor. Measures all intensity noise generated by the EDFA. Disadvantages: If shot-noise-limited source is not available, source output noise must be stable to permit subtraction.

Constant power. Merits: Provides complete noise figure with baseband frequency dependence of noise factor. Measures all intensity noise generated by the EDFA. Disadvantages: If shot-noise-limited source is not available, source output noise must be stable to permit subtraction. Also requires ASE to be small compared to amplified signal.

The ultimate decision on the measurement method will depend on the design and application of the amplifier. Among the optical measurement techniques, the authors have found that the TDE approach combined with a small signal probe and the reduced source technique represents a powerful solution for amplifier characterization. When a measurement of the complete noise figure is required, the optoelectronic methods are employed using the RIN transfer calibration technique.

VII. EDFA TEST SYSTEMS

This paper thus far has focused mainly on the theoretical and measurement methods. The amplifier measurement implementation requires the assembly and coordination of a number of optical and electrical instruments. The response times of each instrument must be carefully synchronized with the rest of the equipment

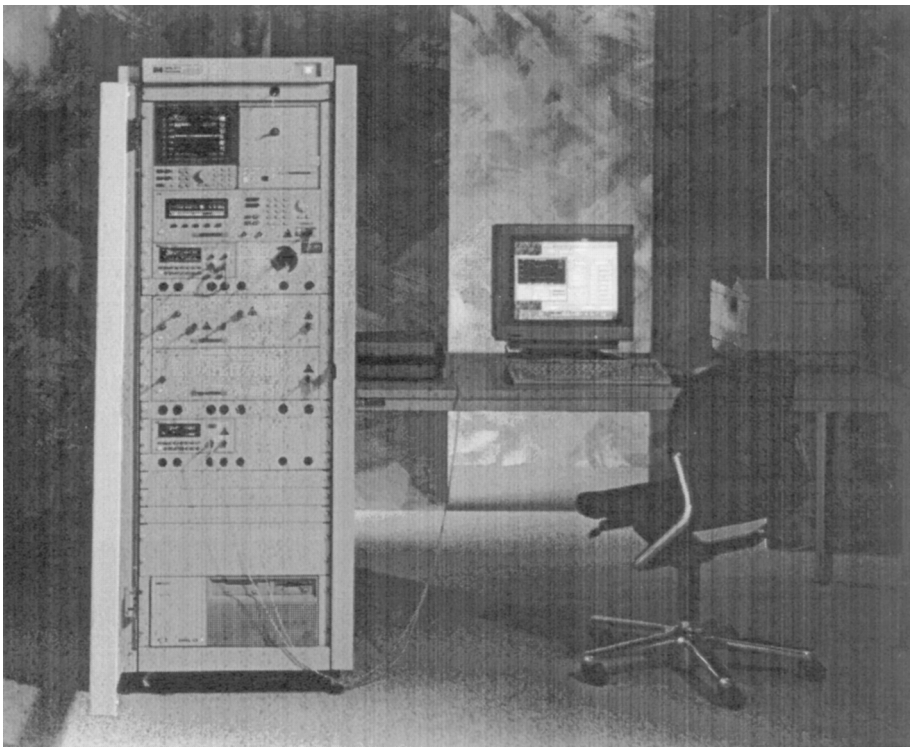

FIG. 20. Photograph of an EDFA test system showing optical instrumentation and computer control and display.

to reduce test time and measurement uncertainty. Often there is a significant amount of software involved to implement the measurement algorithms. An example of an EDFA test system is shown in Fig. 20. In the test rack are lasers for stimulus, optical power meters, an optical spectrum analyzer, and a test set for optical signal processing and supplying and receiving signals from the amplifier under test. A computer is used to control the measurement equipment and process the measured data. Often the measurements are performed over temperature where the amplifier is placed in a temperature-controlled enclosure. When fusion-spliced connections are used, highest measurement accuracy is obtained. A number of the measurement uncertainties are determined by instrumentation limitations such as the polarization dependence of the measurement equipment. Sometimes polarization scrambling is used to reduce this uncertainty. While commercial amplifier test systems offer the convenience a packaged rack-mounted measurement solution, their main contribution lies in the implementation of the measurement algorithms within the context of instrument limitations.

VIII. SUMMARY

A number of different noise mechanisms originating from optical gain, loss, and interference contribute to the total noise figure. A general noise figure formula has

been derived and shown to be consistent with the optical domain and the optoelectronic/electrical domain. The standard signal-spontaneous beat noise factor formula is a direct simplification of the more general relation. The general noise figure formulation requires no assumptions on the types of noise generated by the amplifier.

We have surveyed a number of different measurement techniques. Noise figure can be characterized using either an optical spectrum analyzer or a photodetector followed by an electrical spectrum analyzer. Both methods are based on the same fundamental noise figure definition. Optical methods provide a simple but incomplete characterization of the noise produced by an optical amplifier. However, optical methods do provide an accurate means of obtaining $F_{\text{sig-sp}}$that is useful for cascade calculations of noise figure. Optoelectronic/electrical methods yield complete information on the noise figure but have fewer options for dealing with source excess noise that could easily be mistaken for amplifier-generated noise. Because the optoelectronic/electrical and optical methods are based on the same original noise figure equation, given by Eq. (10), their results compared well in the example at higher baseband frequencies where the effect of the multipath interference is reduced.

REFERENCES

[1] E. Desurvire, *Erbium Doped Fiber Amplifiers, Principles and Application*, Wiley, New York, 1994.

[2] T. Okoshi and K. Kikuchi, *Coherent Optical Fiber Communications*, KTK Scientific, Tokyo, 1988.

[3] D. Derrickson (Ed.), "Characterization of Erbium-Doped Fiber Amplifiers" in *Fiber Optic Test and Measurement*, Chap. 13, Prentice-Hall, Englewood Cliffs, NJ, 1998.

[4] H. A. Haus, "The proper definition of noise figure of optical amplifiers" in *Conference on Optical Fiber Communication-OFC'99*, pp. 310–312, Optical Society of America, Washington, DC, Feb. 1999.

[5] G. P. Agrawal, *Fiber-Optic Communications Systems*, Wiley, New York, 1997.

[6] H. Okamura, "International Standardization of Optical Amplifiers," in *Optical Amplifiers and Their Applications*, paper M3, OAA'99, Optical Society of America, Washington, DC, 1999.

[7] N. A. Olsson, "Lightwave systems with optical amplifiers," *J. Lightwave Technol.*, vol. 7, no. 7, 1071 (1989).

[8] J. L. Gimlett, M. Z. Iqbal, L. Curtis, N. K. Cheung, A. Righetti, F. Fontana, and G. Grasso, "Impact of multiple reflection noise in Gbit/s lightwave systems with optical fiber amplifiers," *Electron. Lett.*, vol. 25, no. 20, 1393 (1989).

[9] J. C. van der Plaats and F. W. Willems, "RIN increase caused by amplified-signal redirected Rayleigh scattering in erbium-doped fibers," in *Conference on Optical Fiber Communication-OFC'94*, 20–25 Feb., pp. 158–160, Optical Society of America, Washington, DC, 1994.

[10] M. N. Zervas and R. I. Laming, "Rayleigh scattering effect on the gain efficiency and noise of erbium-doped fiber amplifiers," *IEEE J. Quant. Electron.*, vol. 31, no. 3, 468 (1995).

[11] J. L. Gimlett, M. Z. Iqbal, N. K. Cheung, A. Righetti, F. Fontana, and G. Grasso, "Observation of equivalent Rayleigh scattering mirrors in lightwave systems with optical amplifiers," *IEEE Photon. Technol. Lett.*, vol. 2, no. 3, 211 (1990).

[12] F. W. Willems, J. C. van der Plaats, C. Hentschel, and E. Leckel, "Optical amplifier noise figure determination by signal RIN subtraction," in *Symposium on Optical Fiber measurements*, NIST Technical Digest, pp. 7–9, 1994.

[13] P. Gallion, J. L. Vey, and F. Jeremie, "Classical optical corpuscular theory of semiconductor laser intensity-squeezed light generation," *Opt. Quant. Electron.*, vol. 29, 65 (1997).

[14] P. Gallion, "A classical corpuscular approach to optical noise," in *Optical Amplifiers and Their Applications*, paper WB2, OAA'99, Optical Society of America, 1999.

[15] M. Movassaghi, M. K. Jackson, V. M. Smith, J. F. Young, and W. J. Hallam, "Noise figure of saturated erbium-doped fiber amplifiers," in *Optical Fiber Communications Conference*, *OFC'97*, OSA Technical Digest Series, vol. 6, pp. 104–105, Optical Society of America, 1997.

[16] F. W. Willems, "The intracacies of an EDFA Round-robin: first observations from COST-241 and RACE 'COMFORT'," in *Symposium on optical fiber measurements*, NIST Technical Digest, pp. 11–14, 1994.

[17] I. Jacobs, "Dependence of optical amplifier noise figure on relative-intensity-noise," *J. Lightwave Technol.*, vol. 13, no. 7, 1461 (1995).

[18] S. Poole, "Noise figure measurement in optical fibre amplifiers," in *Symposium on optical fiber measurements*, NIST Technical Digest, pp. 1–6, 1994.

[19] K. Bertilsson, P. A. Andrekson, and B. E. Olsson, "Noise figure of erbium doped fiber amplifiers in the saturated regime," *IEEE Photon. Technol. Lett.*, vol. 6, no. 10, 199 (1994).

[20] E. Leckel, J. Sang, R. Muller, C. Ruck, and C. Hentschel, "Erbium-doped fiber amplifier test system," *Hewlett-Packard J.*, vol. 46, no. 1, 13 (1995).

[21] G. R. Walker, "Gain and noise characterisation of erbium doped fibre amplifiers," *Electron. Lett.*, vol. 27, no. 9, 744 (1991).

[22] D. M. Baney and R. L. Jungerman, "Optical noise standard for the electrical method of optical amplifier noise figure measurement," in *Optical Amplifiers and Their Applications*, paper MB3, OAA'97, Optical Society of America, Washington, DC, 1997.

[23] G. R. Walker, N. G. Walker, R. C. Steele, M. J. Creaner, and M. C. Brain, "Erbium-doped fiber amplifier cascade for multichannel coherent optical transmission," *J. Lightwave Technol.*, vol. 9, no. 2, 182 (1991).

[24] D. M. Baney and J. Dupre, "Pulsed-source technique for optical amplifier noise figure measurement," *European Conference on Communications*, *ECOC'92*, paper WeP2.11, Berlin, 1992.

[25] H. Chou and J. Stimple, "Inhomogeneous gain saturation of erbium-doped fiber amplifiers," in *Optical Amplifiers and Their Applications*, *OAA'95*, paper ThE1-1, Optical Society of America, Washington, DC, 1995.

[26] C. Hentschel and D. M. Baney, "Signal substitution technique for DWDM optical noise figure measurement," in *Optical Amplifiers and their Applications*, paper TuC5, OAA'98, Optical Society of America, Washington, DC, 1998.

[27] D. M. Baney and J. Stimple, "WDM EDFA gain characterization with a reduced set of saturating channels," *IEEE Photon. Technol. Lett.*, vol. 8, no. 12, 1615 (1996).

[28] F. W. Willems, "Optical amplifier characterization," in *Symposium on optical fiber measurements*, NIST Technical Digest, pp. 17–21, 1996.

[29] E. Rudkevich, D. M. Baney, J. Stimpel, D. Derickson, and G. Wang, "Nonresonant spectral-hole burning in erbium-doped fiber amplifiers," *IEEE Photon. Technol. Lett.*, vol. 11, no. 5, 542 (1999).